Mechanisms of the Reaction of Positive Atomic Oxygen Ions with Nitrogen[1a]

Darrel G. Hopper[1b]

Contribution from the Chemistry Division, Argonne National Laboratory, Argonne, Illinois 60439. Received December 4, 1974 (Revised Manuscript Received September 12, 1977)

Abstract: Mechanisms have been established for the state-to-state reaction $O^+(^4S_u) + N_2(X^1\Sigma_g^+) \rightarrow N(^4S_u) + NO^+(X^1\Sigma^+)$ + 1.1 eV in terms of potential energy hypersurface characteristics for the relevant N_2O^+ electronic states. The surface characteristics are established from ab initio excitation energy calculations at 180° and 130° along with limited scans of the $1^4A''$ potential energy hypersurface. From these results and orbital considerations, adiabatic correlation diagrams are drawn, with emphasis on the quartet states, for $C_{\infty v}$ and C_s symmetry. The main mechanism is then shown to be adiabatic reaction governed by the potential energy hypersurface of the N_2O^+ $1^4A''$ state. The $1^4A''$ state correlates uniquely to the reagents and to the products and presents a minimum energy barrier to reaction of 0.15 ± 0.1 eV at a critical geometry $(R_{NN}^*, R_{NO}^*, A_{NNO}^*) = (1.28 \pm 0.07$ Å, 1.26 ± 0.07 Å, $120 \pm 5°)$. The energy barrier and the extended value of R_{NN}^* relative to the outer anharmonic turning point for $N_2(v)$, $v = 0$ or $v = 1$, 1.15, or 1.18 Å, require that reaction on the $1^4A''$ hypersurface exhibit "threshold" behavior for either translational or vibrational excitation of the reagents. Both of the latter "threshold" effects have been observed in experiments, which, thus, corroborate the present identification of the main mechanism. It is also established that the N_2O^+ quartet states above $1^4A''$ play a net negative role—collisions reaching them tend to yield products other than $N(^4S_u)$ + $NO^+(X^1\Sigma^+)$. A low-energy multistate mechanism is also shown to be possible for this state-to-state reaction: the symmetry-allowed but spin-forbidden process $O^+ + N_2 + M \rightleftharpoons M + N_2\text{-}O^+(1^4A'') \rightarrow N_2O^{+*}(1^2A'') \rightarrow [N\text{-}NO^+(1^4A'')]_{repul} \rightarrow N + NO^+$. The $1^4A''(N_2\text{-}O)^+$ polarization state is shown to have an equilibrium geometry $(R_{NN}^e, R_{NO}^e, A_{NNO}^e) = (1.10 \pm 0.01$ Å, 2.35 ± 0.10 Å, $180°)$ with a binding energy $D^0(N_2\text{-}O^+) = 0.48 \pm 0.1$ eV and $k(N_2\text{-}O^+) = 0.33 \pm 0.05$ mdyn/Å. The minimum in the $1^4A''$-$1^2A''$ N_2-O surface intersection locus occurs at about 0.1 eV below O^+, $N_2(v = 0)$ with $R_{NO} \simeq 1.8$ Å. This low-energy mechanism should predominate below the translational and vibrational thresholds for the single-state $1^4A''$ mechanism. At extremely small translational energies (below about 0.001 eV) a second very low energy mechanism, $O^+ + N_2 \rightarrow N_2O^+(1^2A'') \rightarrow [N\text{-}NO^+(1^4A'')]_{repul} \rightarrow N + NO^+$, can become appreciable.

I. Introduction

The state-specific reaction

$$O^+(^4S_u) + N_2(X^1\Sigma_g^+)$$
$$\rightarrow NO^+(X^1\Sigma^+) + N(^4S_u) + 1.10 \text{ eV} \quad (1)$$
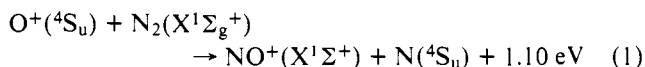
is one of the two ion–molecule reactions most important in determining the properties of the ionosphere.[2] In particular, reaction 1 is the major route for the production of NO^+, which is mainly responsible, via dissociative attachment, for the removal of free electrons and the formation of excited $N(^2D)$.[2-9] The reaction is also an important sink in the set of reactions that determines the vibrational temperature of N_2.[8] Its role in the persistence of O^+ after nightfall has been the subject of considerable discussion.[2-5]

The mechanism for this reaction apparently changes with the relative translational energy E_t of the reagents. The possibility of such changes has also been noted by others.[10-12] For purposes of present discussion, the behavior in the 0 to about 0.1–0.2 eV relative energy range is referred to as the low-energy mechanism(s), the behavior in the 0.1–0.2 to about 10 eV range, the main mechanism(s), and 10 eV up, the high-energy mechanism(s). The similarities and differences of these three mechanisms are discussed in the light of present and other recent results.

The main mechanism may be responsible for virtually all ionospheric NO^+ production via reaction 1. The low-energy mechanism is characterized by a rate coefficient on the order of 10^{-12} cm³/molecule s while the main rate coefficient is up to two orders of magnitude higher.[2-5,10] Contribution from the high-energy mechanism is not significant for temperatures less than 10 000 K. The temperatures in the ionosphere are normally 500–2000 K, but are pushed higher (4000, 8000 K) by perturbing events (e.g., aurora, solar flares).[13] Vibrational excitation of N_2, which would be appreciable under these conditions, has been shown in laboratory experiments to enhance reactivity, especially for temperatures such that vibrational states $v \geq 2$ are appreciably populated but that the relative translational energy is less than 2.5 eV.[6-9,10,14-16] Within the present framework of breaking down the collision energy into low, main, and high ranges, these last mentioned results support the possibility that the reaction enhancement role of vibrational excitation is to energetically enable collisions with relative translational energy in the low range to proceed to reaction via the main mechanism, and to increase the reactivity probability of collisions in the higher energy ranges. The main

Table I. $C_{\infty v}$ SCF Excitation Energies for N_2O^+ Quartet States and the X, A, B, and $1^2\Phi$ Doublet States

| State | Configuration[a] | | | | | | | | Excitation energy, eV[b] | | |
| | 7σ | 8σ | $1\pi_x$ | $2\pi_x$ | $3\pi_x$ | $1\pi_y$ | $2\pi_y$ | $3\pi_y$ | SCF calculation[c] | | Expt[f] |
									Scale 1[d]	Scale 2[e]	Scale 1[d]
$X^2\Pi$	2	0	2	1	0	2	2	0	0.0	−2.6	0.0
$A^2\Sigma^+$	1	0	2	2	0	2	2	0	4.7	2.1	3.65
$1^4\Pi$	2	0	2	1	0	2	1	1	4.5	1.9	4.3
$B^2\Pi$	2	0	2	1	0	2	1	1	5.2	2.6	5.16
$1^2\Phi$	2	0	2	2	1	2	0	0			
	2	0	2	0	1	2	2	0	5.8	3.2	
	2	0	2	1	0	2	1	1			
$1^4\Sigma^+$	1	0	2	1	1	2	2	0			
	+1	0	2	2	0	2	1	1	6.7	4.1	
$1^4\Delta$	1	0	2	1	0	2	2	1			
	−1	0	2	2	1	2	1	0	7.3	4.7	
$2^4\Pi$	2	0	1	1	1	2	2	0	7.6	5.0	
$1^4\Sigma^-$	1	0	2	1	0	2	2	1			
	+1	0	2	2	1	2	1	0	7.9	5.3	
$2^4\Sigma^-$	2	1	2	1	0	2	1	0	9.2	6.6	

[a] The core $1\sigma^2\,2\sigma^2\,3\sigma^2\,4\sigma^2\,5\sigma^2\,6\sigma^2$ is understood. [b] The geometry is the equilibrium geometry of $N_2O(X^1\Sigma^+)$, $R_{NN} = 1.1282$ Å, $R_{NO} = 1.1842$ Å, $A_{NNO} = 180°$. See ref 29. [c] Basis set—Dunning 4s2p contractions of the Huzinaga 9s5p atom-optimized Gaussian sets. See ref 20 and 21. [d] The origin for scale 1 is the total energy of the $X^2\Pi$ state. In the basis set used in this study this energy is -183.1719 au. [e] The origin for scale 2 is the asymptote $O^+(^4S_u)$, $N_2(X^1\Sigma_g^+, v = 0)$. This scale is established from scale 1 by subtracting the experimental dissociation energy of $N_2O^+(X^2\Pi)$ to this asymptote. This dissociation energy is 2.606 eV after removal of the zero-point energies for N_2O^+. See ref 22. [f] From ref 54.

Table II. C_s (130°) SCF Excitation and Bending Energies for N_2O^+

| State | Configuration[a] | | | | | | | Excitation energy, eV,[b] with respect to $X^2\Pi(1^2A')$ at | | Bending energy change, eV |
	$7a'$ $1\pi_x$	$8a'$ 7σ	$9a'$ $2\pi_x$	$10a'$ $3\pi_x$	$1a''$ $1\pi_y$	$2a''$ $2\pi_y$	$3a''$ $3\pi_y$	130°	180°	
$X^2\Pi(1^2A')$	2	2	1	0	2	2	0	0.0	1.2	+1.2
$X^2\Pi(1^2A'')$	2	2	2	0	2	1	0	0.5	1.8	+1.8
$1^4A''(1^4\Pi)$	2	2	1	1	2	1	0	1.5	2.7	−1.8
$2^2A''(B^2\Pi)$	2	2	1	1	2	1	0	2.3	3.5	−1.7
$A^2\Sigma^+(2^2A')$	2	1	2	0	2	2	0	$(3.5)^c$	$(4.7)^c$	$(+1.2)^c$
$1^4\Pi(^4A')$	2	2	1	0	2	1	1	4.3	5.5	+1.0
$B^2\Pi(^2A')$	2	2	1	0	2	1	1	4.9	6.1	+1.2

[a] If more than one spin coupling is possible, all have been included in the calculation. [b] Geometry: $R_{NN} = 1.1282$ Å, $R_{NO} = 1.1842$ Å, $A_{NNO} = 180°$. Basis set: 4s2p (Dunning). Core: $1a'^2\,2a'^2\,3a'^2\,4a'^2\,5a'^2\,6a'^2$. $E_T = -183.1269$ au for $X^2\Pi(1^2A')$ at 130°. [c] Estimated by molecular orbital argument from the N_2O^+ $X^2\Pi(1^2A')$ SCF bending energy.

mechanism is then expected to be the more important one in ionospheric chemistry and is the principal subject of the present discussion. The low-energy mechanism is interesting theoretically in that it is reportedly associated with low albeit finite reactivity below the strong threshold at about 0.15 eV and an inverse temperature dependence from 77 to 700 K.[10,17]

Reaction 1 is somewhat at odds with small gas-phase reaction systems for which the mechanistic behavior is already well understood. The reasons for this notoriety are the switch from inverse to direct temperature dependence on the one hand and the failure of the reaction to exhibit the very high, collision rate limited, thermal reactivity characteristic of many ion–molecule reactions on the other. In this paper the results of ab initio electronic structure calculations for N_2O^+ are reported. Then, a consideration of these new results along with the previous results contained in a companion paper[16] and the extensive literature on reaction 1 is shown to lead to the identification of different dominating mechanisms for the inverse and direct temperature dependencies.

II. Ab Initio Results for N_2O^+

A. Method of Calculation. The ab initio results reported here are from open-shell SCF calculations performed with the computer codes of Das and Wahl[18] and Neumann et al.[19] The one-electron basis sets for nitrogen and oxygen are the Dunning[20] 4s2p contractions of the optimized atomic Gaussian

bases of Huzinaga.[21] The orbitals were optimized separately for the SCF configuration(s) for each state. The configurations are given in Tables I and II.

B. $C_{\infty v}$ Vertical Excitation Energies. The SCF excitation energies to the $1^4\Pi$, $1^4\Sigma^+$, $1^4\Delta$, $2^4\Pi$, $1^4\Sigma^-$, and $2^4\Sigma^-$ quartet states and the $A^2\Sigma^+$, $B^2\Pi$, and $1^2\Phi$ doublet states of N_2O^+ were computed at the experimental equilibrium geometry of N_2O.[22] The latter geometry is very close to that for $N_2O^+(X^2\Pi)$. The results are given in Table I. Where more than one spin coupling is possible, all are included. The excitation energies are given on two scales: scale 1 with respect to the total SCF energy of the $X^2\Pi$ ground state and scale 2 with respect to the $O^+(^4S_u)$, $N_2(X^1\Sigma_g^+)$ asymptotic state. Experimental excitation energies are included for the X, A, and B doublet states for reference. Comparison of the latter experimental values with their SCF counterparts indicates that the uncertainty of the SCF quartet and $^2\Phi$ excitation energies is about 1.0 eV.

C. C_s Vertical Excitation Energies. The $^{2,4}A', A''$ C_s states which correlate to the $C_{\infty v}$ states $X^2\Pi$, $1^4\Pi$, and $B^2\Pi$ have been considered at a valence angle A_{NNO} of 130° with the experimental N_2O bond lengths. The SCF results for these six states are given in Table II along with the configuration optimized.

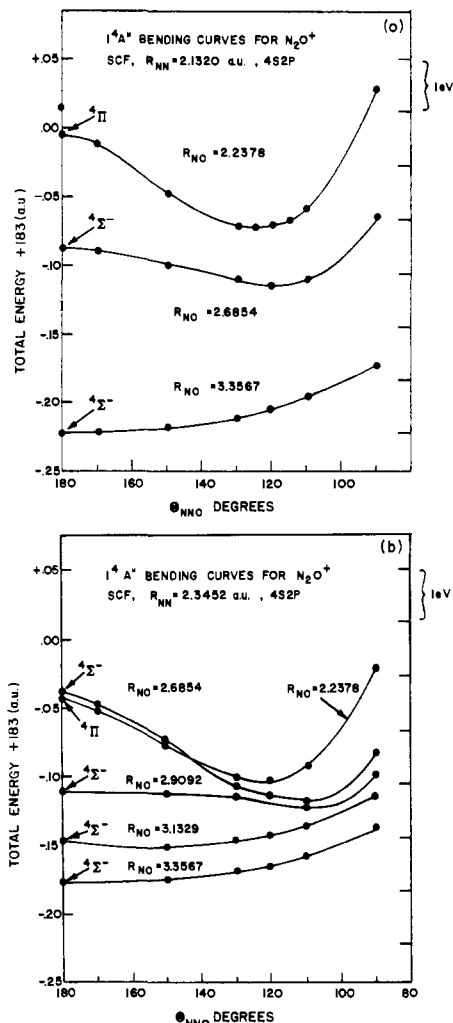An SCF calculation for the $A^2\Sigma^+(^2A')$ state could not be made at 130° because this state differs from $X^2\Pi(^2A')$ by the

Figure 1. Bending curves for $N_2O^+(1^4A'')-(N_2-O)^+$. Length units are au (Å). (a) $R_{NN} = 2.1320$ (1.1282) with $R_{NO} = 2.2378$ (1.1842), 2.6854 (1.4210), or 3.3567 (1.7763). (b) $R_{NN} = 2.3452$ (1.2410) with $R_{NO} = 2.2378$ (1.1842), 2.6854 (1.4210), 2.9092 (1.5395), 3.1329 (1.6579), or 3.3567 (1.7763).

single excitation $8a'^29a' \rightarrow 8a'9a'^2$. A 130° excitation energy of 4.7 eV for $A^2\Sigma^+(^2A')$ with respect to $X^2\Pi$ at 180° is estimated from the experimental 180° excitation energy, 3.5 eV, and the SCF bending energy change for taking $X^2\Pi(^2A')$ from 180° to 130°, 1.2 eV. Such an estimate is deemed reasonable on the basis that the $8a'(2\pi)$ and $9a'(7\sigma)$ orbitals exhibit similar angular dependencies in N_2O.[23]

D. Bending Curves for $N_2O^+(1^4A'')$. Several SCF bending curves from 180° to 90° for the $1^4A''$ state were computed. The results show that the shape and linear state correlation are functions of the bond lengths. Figure 1a presents the curves for $R_{NN} = 2.1320$ au (1.1282 Å) and $R_{NO} = f_{NO} \times 2.2378$ au (1.1842 Å), $f_{NO} = 1.0$, 1.2, and 1.5. Figure 1b presents the curves for a 10% larger value of R_{NN}, 2.3452 au (1.2410 Å), and the five R_{NO} values resulting from $f_{NO} = 1.0$, 1.2, 1.3, 1.4, and 1.5. The linear state correlation is indicated in the figure for each bond length combination. These calculations with R_{NN} at molecule-like values show that the linear state correlation for $1^4A''$ switches from $^4\Sigma^-$ to $^4\Pi$ as R_{NO} decreases from 3.36 au (1.78 Å) to 2.24 au (1.19 A). The $C_{\infty v}$ $^4\Sigma^-/^4\Pi$ intersection occurs at $R_{NO} = 2.6$ au (1.4 Å) for $R_{NN} = 2.13$ au (1.13 Å) or $R_{NN} = 2.35$ au (1.24 Å) in the 4s2p SCF approximation.

Also, these curves demonstrate a change in the minimum-energy valence angle A_{NNO} from 180° to about 120° as $1^4A''(O^+,N_2)$ is brought to $1^4A''(N_2O^+)$. The transition from
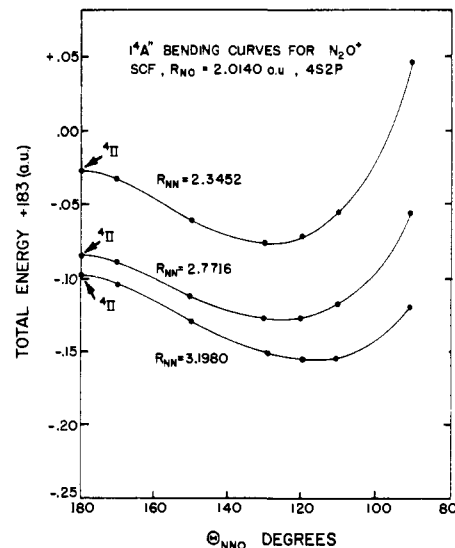

Figure 2. Bending curves for $N_2O^+(1^4A'')-(N-NO)^+$. Length units are au (Å). $R_{NO} = 2.0140$ (1.0658) with $R_{NN} = 2.3452$ (1.2410), 2.7716 (1.4667), or 3.1980 (1.6923).

a linear to a bent valence angle occurs at $R_{NO} = 2.8$ au (1.5 Å) for $R_{NN} = 2.13$ au. An extension of R_{NN} to 2.35 au increases the value of R_{NO} at the transition slightly to 3.0 au (1.6 Å).

Bending curves for the recession of N from NO^+ are presented in Figure 2. The curves shown are for $R_{NN} = f_{NN} \times 2.1320$ au, $f_{NN} = 1.1$, 1.3, 1.5, with $R_{NO} = 2.0140$ au (1.0658 Å). These curves show that the most stable valence angle A_{NNO} decreases steadily as R_{NN} increases.

The preliminary findings of a more extensive SCF survey are that the N—NO^+ bending curves have nonlinear minima at least out to $R_{NN} = 6.4$ au (3.4 Å) and that the most stable angle at long range is $A_{NNO} \simeq 90°$.

For later reference it is noted that the excitation energies given in Table I for the $1^4\Sigma^-$ and $2^4\Sigma^-$ states at $R_{NN} = 2.1320$ au and $R_{NO} = 2.2378$ au are out of the range of Figure 1. These two states would be at +0.11 and +0.15 on the energy scale employed. Also, an examination of the wave functions shows that it is the $2^4\Sigma^-$ state at $R_{NN} = 2.1320$ au and $R_{NO} = 2.2378$ au which has the electronic structure of the long-range $1^4\Sigma^-$ state of Figure 1. Thus, although the total energy for the long-range configuration rises by 0.39 au (11 eV) as R_{NO} decreases from infinity to 2.24 au with $R_{NN} = 2.13$ au, most of the rise—6.5 eV—comes as R_{NO} is decreased the last 0.45 au (0.24 Å).

E. Energy Surface for $N_2O^+(1^4A'')$ at 120°. It has been shown elsewhere that correlated and SCF wave functions for the $1^4A''(1^4\Pi)$ state of N_2O^+ have bending curves which exhibit virtually the same minimum-energy angle.[24] From the SCF bending curves presented above in Figure 1 the geometry along the reaction coordinate for reaction 1 is characterized by a valence angle A_{NNO} in the range 115–125° once R_{NO} has been reduced to a molecule-like value. Thus, an ab initio survey of the short bond length region at an angle of 120° can provide the topology of the $1^4A''$ energy surface in a critical region of the reaction coordinate for reaction 1. Furthermore, the bond length and valence angle relaxation energies can be combined with the correlated ab initio N_2O ionization potential $X^1\Sigma^+$ $\rightarrow 1^4\Pi$ from ref 24 to position the critical region with respect to the atom–diatomic asymptotes of N_2O^+.

In the present study an ab initio SCF survey for $A_{NNO} = 120°$ with double-ζ 4s2p basis set is reported. The coordinate R_{NN} has been varied from 1.0154 Å to 1.4667 Å in steps of 0.11282 Å and the coordinate R_{NO} from 1.0658 Å to 1.7763
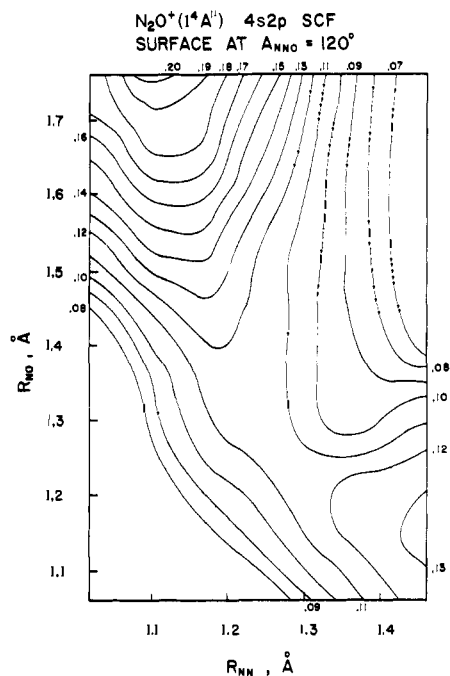
Figure 3. Saddle-point region of the potential energy surface of $N_2O^+(1^4A'')$ at 120°. Contour labels are $-(E_T + 183)$ with the total energy E_T in atomic units.

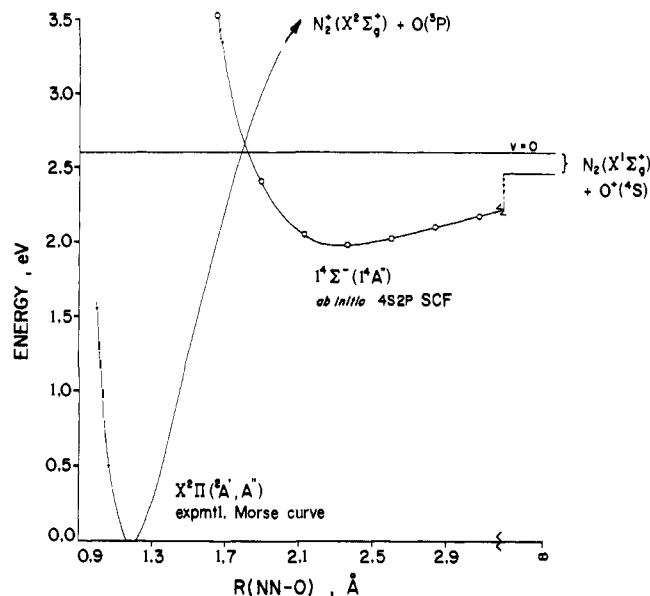

Figure 4. Comparison of the ab initio 4s2p SCF $^4\Sigma^-(1^4A'')$ bonding curve for N_2-O^+ with the $X^2\Pi(1^2A',1^2A'')$ Morse curve for $N_2{}^+$–O.

Å in steps of 0.11842 Å. Figure 3 is a contour plot constructed from the 35 points at which the total energy E_T has been computed. As may be seen from this figure the energy surface exhibits a saddle topology. The saddle point is $R^*_{NN} = 1.28$ Å, $R^*_{NO} = 1.26$ Å, $E^*_T = -183.112$ au. The saddle-point geometry can be estimated to be accurate to ±0.07 Å and ±5° by analogy to the accuracy of the 4s2p SCF geometry for $N_2O^+(X^2\Pi)$.[26]

The potential energy difference E_h between the triatomic saddle point and the asymptote $O^+(^4S_u)$, $N_2(X^1\Sigma_g{}^+)$ is not given accurately from the SCF energy difference between the total energies for the two geometries.[25,26] However, a reliable determination of E_h can be made from the cycle

$$E_h = E^*_T(1^4A'') - E_T(1^4\Pi) + \text{VIP}(X^1\Sigma^+ \to 1^4\Pi)$$
$$- D^0(N_2-O) - \text{IP}(O) \quad (2)$$

The first two terms of eq 2 give the relaxation energy from the equilibrium geometry of $N_2O(X^1\Sigma^+)$ to the minimum energy saddle point for $N_2O^+(1^4A'')$. From the present 4s2p SCF result at 120° this relaxation energy is -2.9 eV. The uncertainty in the latter value is estimated to be 0.1 eV from (a) a comparison of the SCF and correlated bending potentials in ref 24 and (b) the fact that the angle of the minimum SCF saddle-point energy is near but not exactly equal to that of the 120° saddle point. The vertical ionization potential $\text{VIP}(X^1\Sigma^+ \to 1^4\Pi)$ for N_2O is 17.8 eV from a correlated ab initio calculation in which wave functions were separately optimized for the neutral and ion states.[24] The latter value is estimated to be uncertain by 0.6 eV at the level of sophistication at which the calculations were made. Thus, the true vertical position of the $1^4\Pi$ state is expected to be about 18.4 eV, since in the correlated calculations of N_2O excitation energies with a double-ζ plus polarization basis which are currently being made by the author, states obtained from $X^1\Sigma^+$ by excitation of an electron out of the π space come out consistently low, rather than high. The potential energy $D^0(N_2-O)$ for the dissociation of $N_2O(X^1\Sigma^+)$ to $N_2(X^1\Sigma_g{}^+)$, $O(^3P)$ is 1.785 eV.[22-27] The atomic oxygen ionization potential $\text{IP}(O)$ is 13.61 eV.[27] From these values for the terms of eq 2 and their combined uncertainty $E_h = -0.5 \pm 0.7$ eV.

There may be no potential barrier to reaction 1 along the minimum energy pathway. If there is a potential barrier it is no more than 0.1–0.2 eV. Because of the expected direction of the calculated VIP error, it is concluded from these calculations that the true value of E_h is most likely greater than zero.

Further calculations with correlation and a double-ζ plus polarization basis are underway to provide a more accurate value for E_h. The preliminary results yield an $X^2\Pi \to 1^4\Pi$ excitation energy of 5.5 ± 0.3 eV or $E_h = 0.1 \pm 0.4$ eV by a calculation similar to eq 2.

F. Long-Range N_2-O^+ Bonding Curve and $X^2\Pi-1^4\Sigma^-$ Intersection Locus. From classical considerations one expects an attractive portion in the $1^4A''$ potential energy surface as O^+ approaches N_2 from infinity. However, this energy surface is characterized by a saddle-point topology in the short R_{NN}, R_{NO} region. Thus, one expects an intermediate range bond. On the basis of the bending curves shown in Figure 1, the expected N_2-O^+ polarization well will be characterized by an equilibrium bond angle of 180°. It is then the $C_{\infty v}$ state $1^4\Sigma^-(1^4A'')$ which should exhibit the strongest bonding curve in the coordinate R_{NO}. From Figure 1 the minimum is expected to occur at a value for R_{NO} which is greater than 1.7 Å.

In the present work the 4s2p SCF bonding curve for the $1^4\Sigma^-(1^4A'')$ state has been computed for $R_{NO} = 1.7$ Å to $R_{NO} = 3.1$ Å and for $R_{NO} = 118$ Å with $R_{NN} = 1.0976$ Å, the equilibrium bond length of isolated N_2.[26] The resulting curve is plotted in Figure 4. From a power series fit of the computed points the minimum occurs at $R^e_{NO} = 2.35$ Å with a binding energy $D^0(N_2-O^+) = 0.48$ eV and a force constant $k(N_2-O^+) = (\partial^2 V/\partial R_{NO}{}^2)_e = 0.33$ mdyn/Å. Since this well is a result of long-range polarization of a closed-shell molecule (N_2) by a ground state atomic ion (O^+), the SCF calculations should be fairly accurate, even for the binding energy. The preliminary results of more extensive calculations now underway to include polarization basis functions and correlation energy indicate that the currently reported values of R^e_{NO}, $D^0(N_2-O^+)$, and $k(N_2-O^+)$ are accurate to within about ±0.1 Å, ±0.1 eV, and 0.05 mdyn/Å, respectively.

The harmonic stretching frequency for the N_2-O^+ quasi-diatomic is $\omega(N_2-O^+) = 234 \pm 20$ cm^{-1}. As the bending frequency is also very low while the third frequency remains close to that of isolated N_2, the N_2-O^+ potential energy well sup-

Table III. Adiabatic $1\,^4A''$ Reaction Coordinate for $O^+ + N_2 \rightarrow NO^+ + N$

R_{NN}, Å	R_{NO}, Å	A_{NNO}, deg	V, eV	$C_{\infty v}$ state	Comment
1.0976	∞	180	0.0	$^4\Sigma^-$	Reaction coordinate begins $C_{\infty v}$
1.10	2.35 ± 0.1	180	−0.48 ± 0.1	$^4\Sigma^-$	O^+–N_2 polarization well
1.10	1.8 ± 0.1	180	−0.1 ± 0.1	$^4\Sigma^-$	$X^2\Pi$ crossing
1.10	1.8–1.6	180–120	0.0 ± 0.2^a	$^4\Sigma^-$	Reaction coordinate switches to C_s
1.28 ± 0.07	1.26 ± 0.07	120 ± 5	+0.15 ± 0.1	$^4\Pi$	Saddle point
			−0.3 ± 0.2^b	$^4\Pi$	$X^2\Pi(^2A',^2A'')$ crossings
1.8	1.1	115 ± 5		$^4\Pi$	Angle decreases to 115°
3.4 ± 0.2	1.1	90 ± 5	−1.2 ± 0.1	$^4\Sigma^-$	N–NO^+ polarization well
∞	1.0619	90 ± 5	−1.1	$^4\Sigma^-$	Reaction coordinate ends C_s

^{a} Estimated from entries above and below this line. ^{b} Since this is the lowest energy for the doublet–quartet intersection, the value of V at the reaction coordinate is most likely in the upper end of the uncertainty range of this entry.

ports a great many (on the order of 100) closely spaced vibrational states.

Figure 4 includes a Morse curve representation

$$V_M(N_2^+\text{-}O) = D^0(N_2^+\text{-}O)\{1 - \exp[\beta_{NO}R_{NO}']\}^2 \quad (3a)$$

$$R_{NO}' = R_{NO} - R_{NO}^e(X^2\Pi) \quad (3b)$$

of the adiabatic dissociation of $N_2O^+(X^2\Pi)$ to $N_2^+(X^2\Sigma_g^+)$, $O(^3P)$. The parameters for eq 3 are obtained as follows. The N_2^+–O equilibrium bond length $R_{NO}^e(X^2\Pi)$ and binding energy $D^0(N_2^+$–O$)$ for $N_2O^+(X^2\Pi)$ are 1.185 Å and 4.441 eV from the geometry, dissociation energy, frequencies, and ionization potentials for N_2O^+, N_2, and O.[22,27] The $N_2O^+(X^2\Pi)$ force constant k_{NO}^e is 8.35 mdyn/Å.[28] From these values for $D^0(N_2^+$–O$)$ and k_{NO}^e the value of the parameter β_{NO} in eq 3a is 2.429 Å^{-1}.

From Figure 4 the $1\,^4\Sigma^-$–$X^2\Pi$ minimum energy intersection for long R_{NO}, short R_{NN}, occurs for $R_{NO}^{4\rightarrow2} = 1.8$ Å. The linear intersection is the minimum one because the R_{NO} curve for the doublet and, since $R_{NO}^{4\rightarrow2}$ is greater than 1.5 Å, the quarter states rise if the system is bent from 180°. Since the asymptotic values of R_{NN} (1.116 Å for N_2^+ and 1.0976 Å for N_2)[22,27] for the doublet and quartet states are within 0.01 Å of one another, the value at the crossing is expected to be $R_{NN}^{4\rightarrow2} = 1.1$ Å.

A horizontal line is drawn in Figure 4 at the total energy level of O^+, N_2 ($v = 0$). This line is at 2.606 eV with respect to the minimum in the $X^2\Pi$ potential energy well. The $1\,^4\Sigma^-$–$X^2\Pi$ intersection is 0.1 eV above the 2.606-eV line. However, the true $1\,^4\Sigma^-$ curve must be below the 4s2p SCF curve of the present work: the correlation energy should be greater at $R_{NO} = 1.8$ Å than at $R_{NO} = \infty$. Also, the Morse representation of the $X^2\Pi$ adiabatic dissociation to N_2^+,O does not allow for the relaxation of R_{NN} from the molecular equilibrium value, 1.155 Å, to a value near that of N_2^+, 1.116 Å, as R_{NO} increases from 1.185 to 1.8 Å. Although the effects just mentioned will cause relatively small percentage lowerings of the $X^2\Pi$ and $1\,^4\Sigma^-$ curves in the vicinity of their intersection, the potential energy of intersection should drop substantially since the curves meet at a sharp angle. By contrast the distance $R_{NO}^{4\rightarrow2}$ at which intersection occurs should change only minutely.

From these considerations it is concluded that the true $X^2\Pi$ and $1\,^4\Sigma^-$ curves cross at $R_{NO}^{4\rightarrow2} = 1.8 ± 0.1$ Å at a potential energy value *below* the total energy of O^+, N_2 ($v = 0$). Further calculations are underway to verify this conclusion.

G. The $1\,^4A''$ Reaction Coordinate. The SCF results for the $1\,^4A''$ state presented here establish the main features of the geometry of the N_2O^+ system along the minimum energy adiabatic pathway connecting O^+, N_2 to NO^+, N. These features are summarized in Table III. As shown in Table III the SCF reaction coordinate for reaction 1 begins with $A_{NNO} = 180°$ and passes through a linear well minimum at $R_{NO} = 2.4$ Å before crossing the $X^2\Pi$ state at 1.8 Å. Then A_{NNO} drops from 180° to about 120° as R_{NO} decreases through the range

1.8–1.6 Å. To this point R_{NN} has remained within 0.01 Å of its value in N_2, 1.0976 Å.[27] The reaction coordinate then proceeds through a saddle point at about $R_{NN} = 1.28$ Å, $R_{NO} = 1.26$ Å, $A_{NNO} = 120°$. At the saddle point the potential energy in the system is close to the energy of the O^+, N_2 asymptote. As the reaction coordinate descends from the minimum energy saddle point, the valence angle tightens to about $A_{NNO} = 115°$ while R_{NN} extends to 1.8 Å and R_{NO} contracts to 1.1 Å. By the time the system reaches the minimum in the N–NO^+ polarization well at about $R_{NN} = 3.4$ Å, R_{NO} has assumed the value of isolated NO^+ and the valence angle A_{NNO} has decreased to about 90°. The $C_{\infty v}$ state designation to which the $1\,^4A''$ state correlates is $^4\Sigma^-$ except for the region in which the nuclear separations proceed from $(R_{NN}, R_{NO}) = (1.1, 1.6)$ to $(1.8, 1.1)$. In the latter region the linear state to which the $1\,^4A''$ corresponds adiabatically is $1\,^4\Pi$. Thus, the linear state correlation is a function of geometry.

The values entered in the potential column in Table III derive from a critical consideration of the present theoretical and past experimental results. See the Discussion section.

III. Adiabatic Correlation Diagrams for N_2O^+

Many of the states of N_2O^+ might, in general, be accessed during the course of reaction 1. To facilitate the evaluation of the roles of the various N_2O^+ states, $C_{\infty v}$ and C_s adiabatic correlation diagrams are constructed as Figures 5 and 6 from the SCF excitation energies presented in Tables I and II. The ionization potentials and excitation energies necessary to position the atom–diatomic asymptotes of the N_2O^+ system are taken from the literature.[22,27,29] The triatomic states resulting under $C_{\infty v}$ or C_s symmetry from the direct product of each atom–diatom state pair follow from the tables given by Herzberg.[29] The triatomic excitation spectra from Tables I and II are placed in the center of each diagram by positioning the $N_2O^+(X^2\Pi)$ state at experimental ionization potential for N_2O. Although information exists on the position of some of the doublet states above $1\,^2\Phi$, these states are not included in order to avoid congestion.[26,30] It will be shown below that these higher doublets may be neglected in the discussion of mechanisms for reaction 1.

Figure 6 includes several excited C_s quartet states which are not positioned on the basis of the 130° SCF calculations given in Table II. These states are estimated from the 180° SCF calculations of Table I (for the $1\,^4\Sigma^+$, $1\,^4\Delta$, $2\,^4\Pi$, $1\,^4\Sigma^-$, and $2\,^4\Sigma^-$ states) by the following consideration of the effects of electon correlation energy and bending upon the $C_{\infty v}$ excitation energies.

The correlation of the wave functions for the lower excited states of N_2O has been shown to increase their excitation energies from the SCF values if the number of π electrons is the same for the ground and excited states.[26] Thus, one might reasonably expect that the electron correlation energy corrections for the $1\,^4\Pi$, $2\,^4\Pi$, and $2\,^4\Sigma^-$ SCF excitation energies would raise them somewhat. Indeed, from correlated calculations now in progress by the author the correlated excitation
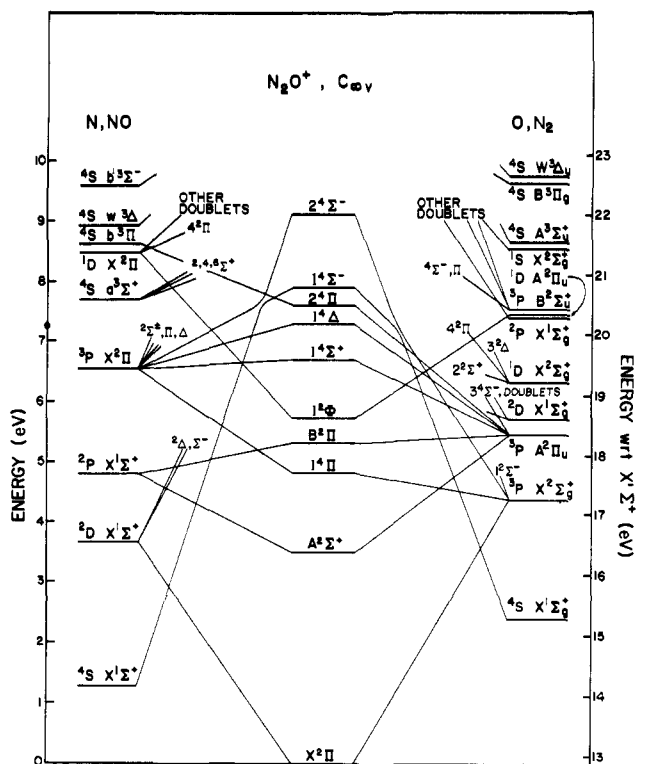
Figure 5. $C_{\infty v}$ adiabatic correlation diagram for N_2O^+ with emphasis on the quartet states. The nuclear separations R_{NN} and R_{NO} are the equilibrium values for N_2O.

Figure 6. C_s adiabatic correlation diagram for N_2O^+ at 130° for the lowest few states. The nuclear separations R_{NN} and R_{NO} are the equilibrium values for N_2O. Emphasis is on quartet states.

energy of the $1^4\Pi$ state with respect to the $X^2\Pi$ state is 5.5 eV, or 1.0 eV above the SCF result of Table I. Similar correlation corrections of +1.0 eV are assumed for the $2^4\Pi$ and $2^4\Sigma^-$ states.

The $1^4\Sigma^+$, $1^4\Delta$, and $1^4\Sigma^-$ states in Table II are obtained from the $X^2\Pi$ state by a $\sigma \rightarrow \pi$ electron transition. This transition may be visualized as the orbital excitation $7\sigma^2 \rightarrow 7\sigma\, 3\pi$. The $A^2\Sigma^+$ state is obtained from the $X^2\Pi$ by the orbital excitation $7\sigma^2\, 2\pi^3 \rightarrow 7\sigma\, 2\pi^4$. The SCF result for the latter excitation is 1.0 eV above the experimental value.[29] In the absence of further information the correlation correction for the $1^4\Sigma^+$, $1^4\Delta$, and $1^4\Sigma^-$ states are taken to be about -1.0 eV by analogy to the $A^2\Sigma^+$ state where a $7\sigma \rightarrow n\pi$ transition also occurs.

One or another of the above-listed $C_{\infty v}$ quartet states results upon raising the angle A_{NNO} to 180° for a bent N_2O^+ molecule in one of the nine C_s states $1-4^4A'$, $1-5^4A''$. As shown in Table II the lowest quartet state, $1^4A''(1^4\Pi)$, is stabilized with respect to linearity by about 1.8 eV. This stabilization upon bending to a C_s nuclear conformation correlates with the occupancy of the $10a'$ orbital.[24] A consideration of the lack of occupancy of the $10a'$ orbital for the $^4A'$ component of the $1^4\Pi$ leads one to expect that this $^4A'$ state will not be stabilized significantly upon bending from 180° but rather destabilized. Indeed, an SCF calculation for the $1^4\Pi(^4A')$ state at 130° yields a total energy which is 1.0 eV above the value at 180° as shown in Table II. One can extend the $10a'$ orbital analysis to estimate bending effects for the higher quartet states. On the basis of the magnitude of the energy changes resulting from bending the $^4A''$ component of the $1^4\Pi$ state from 180° to 130° the stabilization of the $^4A'(1^4\Sigma^+)$, $^4A'(1^4\Delta)$, $^4A''(^4\Delta)$, $^4A'$-$(2^4\Pi)$, and $^4A''(1^4\Sigma^-)$ upon similar bending is estimated to be about 1.8 eV or less. Similarly, the $2^4\Pi(^4A'')$ and $2^4\Sigma^-(^4A'')$ states should rise about 1 eV upon bending from 180° to 130° by analogy to the $1^4\Pi(^4A')$ result.

Application of the correlation and bending energy changes estimated above to the scale 1 entries of Table I yields the C_s (130°) positions of the excited quartet states with respect to
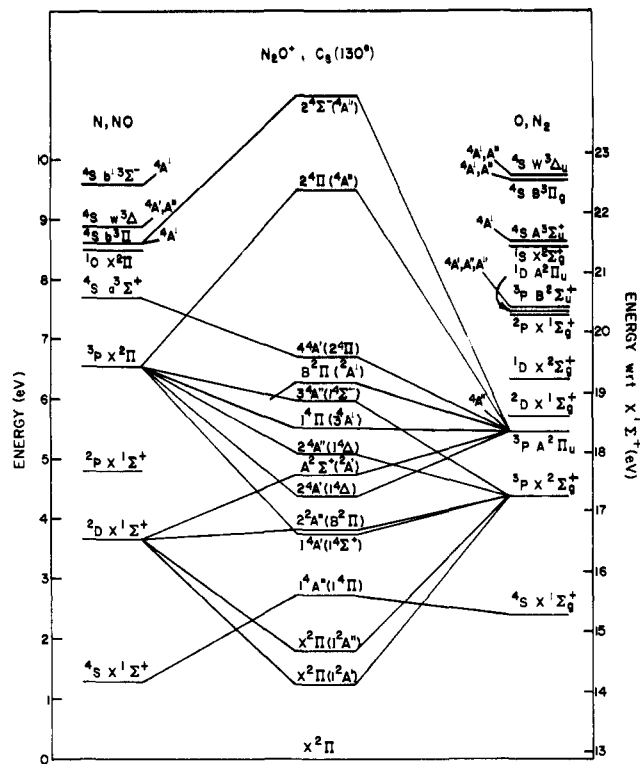
$N_2O^+(X^2\Pi)$. The results are 3.8, 4.4, 5.0, 6.0, 6.4, 6.7, 9.5, and 11.1 eV for the $^4A'(1^4\Sigma^+)$, $^4A'(^4\Delta)$, $^4A''(^4\Delta)$, $^4A''(1^4\Sigma^-)$, $^4A'(1^4\Pi)$, $^4A'(2^4\Pi)$, $2^4\Pi(^4A'')$, and $2^4\Sigma^-(^4A'')$ states, respectively. The $^4A''(^4\Delta)$ state has one more electron in an orbital of a' symmetry than does the $^4A'(^4\Delta)$ state; therefore, the former has been adjusted upwards from 1.9 eV by 0.6 eV. The latter value is the C_s splitting between the $X^2\Pi$ components at 130° where the same situation occurs with regard to the number of electrons in a' orbitals.

Note that the opposing directions of correlation corrections place the $^4A'(1^4\Sigma^+)$ and $^4A'(1^4\Delta)$ states below the $1^4\Pi(^4A')$. This shift is enabled by the opposite directions of the bending energy changes. Note also that the second lowest quartet state is more than 1 eV above the $1^4A''(1^4\Pi)$ state. Similarly, the only doublet states close to the $1^4A''$ state are the $X^2\Pi(1^2A')$ and $X^2\Pi(1^2A'')$, each of which the $1^4A''$ crosses twice.

IV. Evaluation of the Roles of N_2O^+ States in Reaction 1

A. Lowest Quartet State. From the ab initio results presented here and elsewhere[24] it is clear that the lowest quartet state of N_2O^+ provides a low-lying, electronically adiabatic pathway the mechanism

$$O^+ + N_2 \rightarrow [N_2O^+] \rightarrow NO^+ + N$$
$$1^4\Sigma^-(1^4A'') \quad 1^4A''(1^4\Pi) \quad 1^4A''(1^4\Sigma^-) \qquad (4)$$
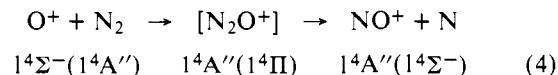
for reaction 1. The availability of this pathway is also obvious from the C_s state correlation diagram, Figure 6. In the present work the reaction coordinate for this pathway is shown to pass through a minimum energy saddle point $R^*_{NN} = 1.28 \pm 0.07$ Å, $R^*_{NO} = 1.26 \pm 0.07$ Å, $A^*_{NNO} = 120 \pm 5°$. The potential energy barrier at this critical geometry to the reagents $O^+ + N_2$ is 0.1 ± 0.4 eV, according to the best ab initio excitation calculations completed as of this writing. The position of the saddle point in the (R_{NN}, R_{NO}) plane indicates that vibrational excitation of N_2 will facilitate reaction via the adiabatic mechanism given in eq 4. This point is made clear by the fact
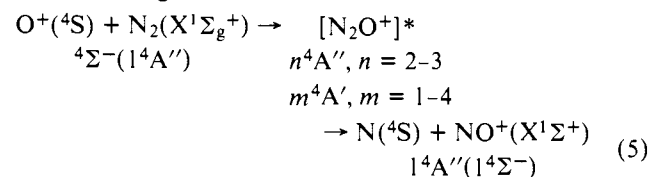
that the N–N separation at the 120° SCF saddle point, 1.28 ± 0.07 Å, is significantly greater than the outer anharmonic classical turning points of isolated $N_2(v)$, $v = 0$–1. Thus, mechanism 4 can contribute to reaction 1 if (a) the translational energy is sufficient to overcome the barrier for $N_2(v = 0)$ or if (b) the nitrogen is excited vibrationally for low translational energies.

B. Excited Quartet States. A consideration of excited quartet states is necessary in any comprehensive attempt to understand the mechanisms for reaction 1 at collision energies in the electron volt region. It is noted at the outset of this consideration that reaction 1 requires the production of ground electronic state products $N(^4S)$, $NO^+(X^1\Sigma^+)$ from the reactants $O^+(^4S)$, $N_2(X^1\Sigma_g^+)$. Furthermore, the term "excited quartet state" in the present context refers to a quartet state other than the $1^4A''$ in which reaction 1 begins and ends.

From Figures 5 and 6 the second $^4A''$ state in N_2O^+ is identified as the C_s state $2^4A''(1^4\Delta)$. The minimum in the energy surface for this state lies about 2.6 eV above the $O^+ + N_2$ asymptote, which is to be compared with the placement of the saddle point in the $1^4A''$ surface at 0.1 eV above the same reagents. The lowest $^4A'$ state is identified as $1^4A'(1^4\Sigma^+)$ at about 1.3 eV above $O^+ + N_2$. It is concluded on energetic considerations alone that higher quartet states play no role in either the low-energy mechanism below 0.1 eV relative energy or the principal mechanism responsible for strong threshold behavior which begins at about 0.1 eV.

For collision energies of 1.3–8 eV and up the reactants $O^+(^4S)$, $N_2(X^1\Sigma_g^+)$ have sufficient energy to reach the bent excited triatomic quartet states. See Figure 6. However, the first excited quartet states having the symmetry of the reactants are the $2^4A''(1^4\Delta)$ and $3^4A''(1^4\Sigma^-)$ whose C_s (130°) minima are about 2.5 and 3.5 eV above the saddle point in the $1^4A''(1^4\Pi)$ surface. All of the surfaces for these three states are expected to rise with angle changes from their C_s minima. Thus, the lowest energy avoided crossing of the $1^4A''$ surface with the surfaces of the strongly bent n^4A'' quartet states is at least 4–5 eV.

Should a collision with relative energy above 4–5 eV take the system to these avoided intersections and, thence, to any of the excited quartet states, the collision cannot lead to ground-state products $N(^4S)$, $NO^+(X^1\Sigma^+)$ except by returning to the $1^4A''$ state. From Figure 6 it is seen that trajectories reaching these excited quartet states would lead to the adiabatic production of excited atom–diatomic asymptotes such as $N^+(^3P)$, $NO(X^2\Pi)$, $O(^3P)$, $N_2^+(X^2\Sigma_g^+)$, and $O(^3P)$, $N_2^+(A^2\Pi_u)$. The probability that reaction 1 proceeds via dual sets of crossings

$$
\begin{array}{cc}
O^+(^4S) + N_2(X^1\Sigma_g^+) \rightarrow & [N_2O^+]^* \\
{}^4\Sigma^-(1^4A'') & n^4A'', n = 2\text{--}3 \\
& m^4A', m = 1\text{--}4 \\
& \rightarrow N(^4S) + NO^+(X^1\Sigma^+) \\
& 1^4A''(1^4\Sigma^-)
\end{array} \quad (5)
$$

is considered to be relatively low for two reasons. First is the steric factor. Triatomic avoided intersections are often quite localized.[31,32] Nonetheless, passage through just one avoided intersection would not necessarily make a process improbable. But mechanism 5 would require the system to pass through the appropriate configurations of *one or more* avoided intersections as O^+ approaches N_2 *and* then through *others* as N recedes in order to yield $N(^4S)$, $NO^+(X^1\Sigma^+)$, rather than one of the excited atom–diatomic asymptotes. The second reason is that the probability of a successful transition is less than unity at each of the several avoided intersections along the way.
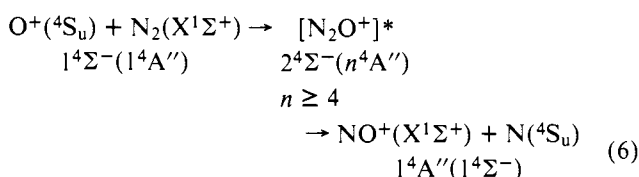
The same arguments against reaction via the excited $^4A''$ states apply to the $^4A'$ states as well. The additional symmetry restriction against a $^4A'' \rightarrow {}^4A'$ transition makes the partici-

pation of the $^4A'$ states in any mechanism for reaction 1 more improbable.

Thus, the more important role of the strongly bent lower quartet states with regard to reaction 1 would appear to be the production of excited (with respect to $O^+(^4S)$, $N_2(X^1\Sigma_g^+)$ or $N(^4S)$, $NO^+(X^1\Sigma^+)$ atom–diatomic asymptotes at the expense of $N(^4S)$, $NO^+(X^1\Sigma^+)$ production via mechanism 4.

One of the lowest quartet avoided crossing is expected to be the avoided intersection of the reagent $^4\Sigma^-(^4A'')$ with the $^4A''(^4\Pi)$ at an angle just less than 180°. This avoided crossing occurs near in energy to the 180° $^4\Sigma^-$–$^4\Pi$ crossing at about 2.5 eV. However, only those O^+, N_2 collisions having total energy resonant with this near crossing should be expected to maximize the probability of the electronic structure change $^4\Sigma^-(^4A'') \rightarrow {}^4A''(1^4\Pi)$. A sharp change in the $10a'$ orbital is observed at 170° in SCF calculations which are underway for the linear intersection locus. The changes are smooth and gradual at 150° and larger angles. If the structure change does occur on a given collision one has the near-180° version of the adiabatic mechanism 4.

Linear and near-linear collisions with sufficient energy may cause the system to retain the long-range electronic structure of the O^+, N_2 asymptotic $^4\Sigma^-(^4A'')$. In the triatomic region it is the $2^4\Sigma^-$ state at about 6.5 eV above O^+, N_2 which has the electronic structure of the reagent $^4\Sigma^-$ state. Thus, for collision energies above about 6.5 eV one expects that linear and near-linear collisions could proceed diabatically to $N(^4S)$, $NO^+(X^1\Sigma^+)$ from the reagent asymptotic $^4\Sigma^-$ surface through crossings and avoided intersections with the $1^4\Pi$, $1^4\Delta$, $2^4\Pi$, and $1^4\Sigma^-$ triatomic states:
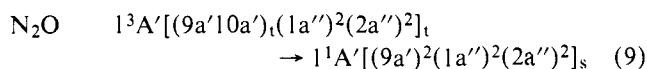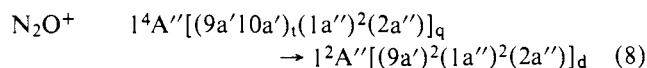
$$
\begin{array}{cc}
O^+(^4S_u) + N_2(X^1\Sigma^+) \rightarrow & [N_2O^+]^* \\
1^4\Sigma^-(1^4A'') & 2^4\Sigma^-(n^4A'') \\
& n \geq 4 \\
& \rightarrow NO^+(X^1\Sigma^+) + N(^4S_u) \\
& 1^4A''(1^4\Sigma^-)
\end{array} \quad (6)
$$

However, the rotational motion of N_2, the randomness of the plane of that motion with respect to the approach velocity vector for O^+, and the low probability of a zero impact parameter combine to make collinear and near-collinear collisions relatively improbable. Thus mechanism 6 is expected to be much less important than mechanism 4, even for collision energy greater than about 6.5 eV. It is more probable that reactive linear collisions beginning on the $1^4\Sigma^-$ surface will produce the charge exchange asymptotes $O(^3P)$, $N_2^+(X^2\Sigma_g^+$ or $A^2\Pi_u)$ via crossings to the $2^4\Sigma^-$ and $3^4\Sigma^-$ $C_{\infty v}$ states arising from these asymptotes. Again one has a net negative role for the excited quartet states insofar as reaction 1 is concerned.

C. Doublet States. An understanding of the mechanisms for reaction 1 must involve too a consideration of the doublet states of N_2O^+. The first strike against the participation of the doublet states is that transition to them from the $1^4A''$ reagent state is spin forbidden. The probability of crossing from the $1^4A''$ to the $1^2A''$ surface upon a single passage of the system through the intersection shown schematically in Figure 6 can be estimated with the one-dimensional Landau–Zener formula

$$
P = 1 - \exp(-A/E_t^{1/2}) \quad (7)
$$

for the transition probability P.[33-35] In eq 7, A is the coupling strength and E_t is the translational energy. The one dimension considered is taken here to be the motion of the atomic oxygen ion with respect to nitrogen. The coupling strength is assumed to be 0.025 $(\text{kcal/mol})^{1/2}$, the value deduced by Tully[32] in the analogous spin-forbidden unimolecular decomposition of nitrous oxide to an oxygen atom and nitrogen. The analogy is quite close. The N_2O unimolecular decomposition involves oxygen atom motion with respect to nitrogen at the crossing
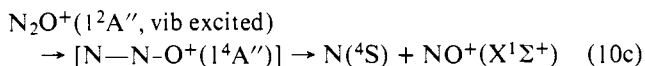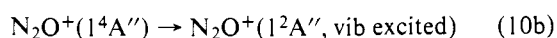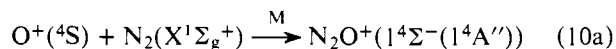
of the $1^1A'$ and $1^3A'$ potential surfaces and in both cases the spin-forbidden transition involves the single spin-orbital excitation $(9a')_s^2 \rightarrow (9a'10a')_t$:

$$N_2O^+ \quad 1^4A''[(9a'10a')_t(1a'')^2(2a'')]_q$$
$$\rightarrow 1^2A''[(9a')^2(1a'')^2(2a'')]_d \quad (8)$$

$$N_2O \quad 1^3A'[(9a'10a')_t(1a'')^2(2a'')^2]_t$$
$$\rightarrow 1^1A'[(9a')^2(1a'')^2(2a'')^2]_s \quad (9)$$

In eq 8 and 9 the subscripts s, d, t, and q represent singlet, doublet, triplet, and quartet spin coupling, respectively. The transition probability is then 0.0338 at 0.001 eV, 0.0108 at 0.01 eV, 0.0034 at 0.1 eV, 0.0011 at 1.0 eV, and 0.000 04 at 7 eV. The probability at the last energy compares with a reactive fraction of 0.310 at 7.0 eV found in a trajectory study on a surrogate adiabatic surface.[15,16] The cross section from the trajectory study at 7.0 eV is slightly less than the experimental values at that energy. Thus, reaction via a doublet state for a collision energy in the 0.1–10-eV range is 100–10 000 times less probable than adiabatic reaction (mechanism 4).

This spin-orbit situation alone rules out a significant role for all doublet states of N_2O^+ except the $X^2\Pi(1^2A'$, and $1^2A'')$. These two doublet states can be reached at low collision energies in the 0–0.1-eV range via the short R_{NN}, long R_{NO} crossing of the $X^2\Pi$ and $^4\Sigma^-$ states. As shown in Figure 4 and in the discussion associated with its presentation in the ab initio results section, this crossing occurs at or below the O^+, $N_2(v = 0)$ asymptote.

The existence of the $(N_2-O)^+$ well for the $1^4\Sigma^-(1^4A'')$ state reported in Figure 4 and the fact that this well is crossed by the $X^2\Pi(1^2A'')$ curve at or below the O^+, $N_2(v = 0)$ level suggests the following three-step mechanism involving the $X^2\Pi(1^2A'')$ state:

$$O^+(^4S) + N_2(X^1\Sigma_g^+) \xrightarrow{M} N_2O^+(1^4\Sigma^-(1^4A'')) \quad (10a)$$

$$N_2O^+(1^4A'') \rightarrow N_2O^+(1^2A'', \text{vib excited}) \quad (10b)$$

$$N_2O^+(1^2A'', \text{vib excited})$$
$$\rightarrow [N-N-O^+(1^4A'')] \rightarrow N(^4S) + NO^+(X^1\Sigma^+) \quad (10c)$$

The existence of the well in the quartet surface enables step 10a to occur. The formation of a stable molecule $N_2O^+(1^4A'')$ in a potential well crossed by the $X^2\Pi(1^2A'')$ potential surface enables an appreciable rate for step 10b. Step 10b occurs via the spin-orbital transition $(9a'10a')_t \rightarrow (9a')^2$. Even though the single pass probability for this spin-orbital transition is shown in a previous paragraph to rise to 0.03 as the translational energy falls to 0.001 eV, it is not sufficiently high to cause a direct mechanism

$$O^+(^4S) + N_2(X^1\Sigma^+) \rightarrow N_2O^+(X^2\Pi) \rightarrow N(^4S)$$
$$+ NO^+(X^1\Sigma^+) \quad (11)$$
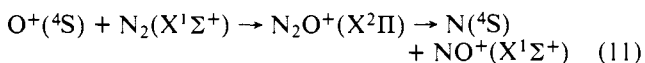
to be significant compared to mechanism 10. Mechanism 10, step b, allows the low probability of the quartet-doublet transition to be overridden in that it provides for a multiple passage of the system through the $1^4A''-1^2A''$ intersection via the vibrational motion of $N_2O^+(1^4A'')$. Step 10c consists of the spin-orbit transition $(9a')^2 \rightarrow (9a'10a')_t$ at the repulsive $N-NO^+$ side of the $1^4A''$ potential surface. Since the SCF bending curves in Figure 2 and the 120° surface scan in Figure 3 show the $1^4A''$ surface to fall monotonically as N separates from NO^+, it is expected that the $1^2A''-1^4A''$ crossing for long R_{NN}, short R_{NO} occurs below the saddle point. From this qualitative surface information and the placement of the saddle point at about 0.1 eV above O^+, N_2 in section II, the $1^2A''-1^4A''$ crossing leading to N, NO^+ occurs at or below the potential energy of O^+, N_2.

Table IV. Mechanisms of the State-Specific Reaction $O^+(^4S_u) + N_2(X^1\Sigma_g^+) \rightarrow NO^+(X^1\Sigma^+) + N(^4S_u)$

E_t, eV	Nitrogen vibrational state	Text equation no. Principal mechanism	Text equation no. Secondary mechanism(s)
0–0.1	≤1	(10)	(11) if $E_t < 0.001$
0–0.1	≥2	(4)	(10)
0.1–10		(4)	(6) if $E_t > 6.5$, (10)
10–25		(4)	CID,[a] (6)
25 and up		CID[a]	(4)

[a] Collision-induced dissociation (CID) becomes important at 12 eV and dominant above about 25 eV.[15,16]

Mechanism 10 is, in summary, expected to be the most important mechanism involving doublet states. However, even mechanism 10 should be of minor importance relative to mechanism 4 for $E_T > E_a \simeq 0.1$ eV or $v > 2$: the N_2-O^+ potential well is just 0.5 eV deep. Collision energies $> E_a$ do not permit time for third body stabilization and the well can only hold two vibrational quanta in N_2.

Mechanism 11 for direct reaction via the $X^2\Pi$ without the initial formation of $N_2O^+(1^4A'')$ is not expected to be important relative to mechanism 10 for collision energies above 0.001–0.01 eV. Note that mechanism 10 is symmetry allowed at nonlinear conformations and that the bending potential favoring 180° is weak at the extended value of R_{NO} at which the doublet-quartet surface crossing occurs.

V. Discussion

In the present article mechanisms for reaction 1 have been suggested on the basis of the characteristics of the potential energy surfaces of N_2O^+. These mechanisms are summarized in Table IV. The potential energy surface information required is provided by the ab initio results and other theoretical considerations reported above. A discussion of these mechanisms in relation to the experimental information on reaction 1 is now presented.

The evidence of the present study requires the conclusion that the main route by which reaction 1 can proceed is mechanism 4—adiabatic reaction on the $1^4A''$ potential energy hypersurface. The ab initio results yield a potential energy barrier E_h of -0.5 ± 0.7 eV presently and 0.1 ± 0.4 eV in correlated work currently underway. From qualitative considerations one expects that the translational cross section $\sigma(E_t)$ for mechanism 4 with thermal N_2 will exhibit a threshold at $E_t \simeq E_h$, rise to a peak, and then fall off as the translational energy E_t goes from zero to infinity. Such behavior for $\sigma(E_t)$ has been illustrated quantitatively for the T + H_2[36] and F + H_2[37] barrier surface reactions and it has been observed for reaction 1.[3,6,7,17,38–43] The experimental results show a translational onset E_a for threshold behavior at 0.15 ± 0.05 eV.[10,17,39,43] This experimental onset is interpreted here to provide a more precise value for E_h, 0.15 ± 0.1 eV, from the relationship

$$E_h = E_a - \epsilon^* + \epsilon(N_2) \quad (12)$$

if the minimum vibrational energy ϵ^* of $N_2O^+(1^4A'')$ at the saddle-point geometry is estimated to be within 0.05 eV of that of isolated nitrogen, $\epsilon(N_2)$. The ab initio results also show that the adiabatic pathway is available for translational energies $E_t < E_h$ if the nitrogen is vibrationally excited. The latter result follows from the present value of R_{NN}^*, 1.28 ± 0.07 Å. A nitrogen molecule in just the first vibrationally excited state N_2 ($v = 1$) provides the system with more than enough total energy to surmount the potential energy barrier, E_h, but not enough N-N motion to take R_{NN} to R_{NN}^*. The N_2 vibrational cross section $\sigma(v)$ for reaction 1 has been found experimentally to rise by over an order of magnitude beginning at $v = 2$ and

leveling off at $v = 5$–6.[6,7] The vibrational enhancement becomes negligible by the time $E_t > E_h + 0.8$ eV, as expected qualitatively and as has been observed for reaction 1, in particular, in experimental,[14] trajectory,[15,16] and semiempirical modeling[44] studies. The presence of a potential energy barrier in the $1^4A''$ surface requires, by analogy to neutral barrier reactions (see, e.g., ref 37), that the differential cross section exhibit backward peaking for E_t just above E_h and then move forward of 90° as E_t increases. Because of the difficulty associated with the reliable detection of low-velocity, backward-scattered product ions from low-energy ($E_t < 4$ eV)[45] ion–molecule collisions in a crossed-beam experiment,[42,45,46] the most trustworthy evidence on the differential cross section below 4 eV relative energy is from a merged-beam experiment.[41] The latter experiment gave predominantly backward scattering at $E_t = 1$ eV and forward at $E_t = 9$ eV. This behavior has been corroborated by a trajectory study for reaction 1 which places the switch from backward peaking to forward peaking at 2–3 eV.[15,16] Very recent studies on autoionizing N_2O^+ Rydberg states below $N_2O^+(A^2\Sigma^+)$ have been found to yield NO^+ at a threshold of 14.8 eV above N_2O, or 0.5 eV below the asymptotic state $O^+(^4S)$, $N_2(X^1\Sigma_g^+)$.[47] Since a reasonable interpretation of the NO^+ appearance is from orbital reclassification in C_s symmetry at 180° followed by orbital ordering changes upon bending

$$(7\sigma)(2\pi)^4(R) \xrightarrow{180°} (8a')(9a')^2(2a'')^2(R)$$

$$\xrightarrow{<180°} (8a')^2(9a')(2a'')^2(R)$$
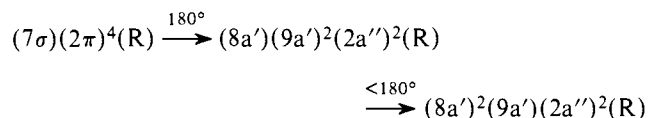
where R represents the Rydberg orbital, followed by a two-electron process to yield $(8a')^2(9a')(10a')(2a'') + e$, one has possibly direct spectroscopic evidence for the low-lying $1^4A''$ state. That the threshold for NO^+ appearance is below the 120° saddle point is consistent with the rapid fall-off of the surface from the saddle point at all angles.

The results of the present study also lead to the conclusion that the dominant mechanism for reaction 1 if $E_t < E_h$ and N_2 ($v = 0, 1$) is mechanism 10—collisional stabilization into the $1^4\Sigma^-(1^4A'')$ N_2–O^+ potential well which is *preassociated* by the $X^2\Pi(1^2A'')$ energy surface which is *predissociated* to products by the $1^4A''(1^4\Pi)$ N–NO^+ energy surface. Since it is the first step which is rate limiting in mechanism 10 and since the inverse of this step (collision-induced dissociation) becomes more important as the relative energy rises, the rate for reaction via mechanism 10 is expected to decrease as the relative energy increases.[48] This sort of behavior has been observed for reaction 1 in the form of an inverse temperature dependence for the reaction rate from 82 K to 700 K.[10,17,43] Furthermore, the third-body stabilization required in step 10a requires a positive pressure dependence for the reaction rate. Such a pressure dependence has been observed for reaction 1 at 82 K but not at 280 K.[9] The latter result is taken here to imply that mechanism step 10a and its inverse are roughly equivalent in rate at 280 K, i.e., that the collision energies are high enough that the third body is as likely to dissociate the nascent N_2–O^+ collision complex as to stabilize it to N_2O^+ in the $(NN-O)^+$ well of the $1^4\Sigma^-(1^4A'')$ electronic state. It is recognized that mechanism 10 would yield $N_2O^+(X^2\Pi)$, vibrationally excited, as an intermediate and that N_2O^+ has not been observed at low temperature.[9] However, this negative result is no surprise since the various low-temperature experiments which have been reported involve reaction times before sampling which are on the order of milliseconds[9] whereas the lifetime for mechanism step 10c is on the order of microseconds. Ionization studies on N_2O give a lifetime of 0.54 μs for the dissociation of $N_2O^+(X^2\Pi)$, vibrationally excited, to $NO^+(X^1\Sigma^+ + N(^4S))$.[49] Furthermore, the sharp peak at 0.8 ± 0.2 eV relative energy

for the products $N + NO^+$ from photoionization and electron-impact studies of N_2O is interpreted here as a placement of the minimum in the intersection locus of the potential energy surfaces for the $X^2\Pi(1^2A'')$ and $1^4A''(1^4\Pi)$ potential energy surfaces.[49–52] This minimum energy crossing occurs, then, at -0.3 ± 0.2 eV with respect to the potential energy of the $O^+(^4S)$, $N_2(X^1\Sigma_g^+)$ asymptote. The observation of O^+ signal appearance at the thermodynamic threshold in the electron impact studies is in agreement with the placement in the present study of the $X^2\Pi(1^2A'')$–$1^4\Sigma^-(1^4A'')$ crossing for long R_{NO} at just below the $O^+(^4S)$, $N_2(X^1\Sigma_g^+, v = 0)$ asymptote. The present mechanism 10 is seen to be similar to but more detailed than the low-temperature mechanism proposed by Ferguson et al.[4,5,53]

In a previous section it is suggested that the contribution of mechanism 5—spin, symmetry, and for $E_t > 2.6$ eV energetically allowed reaction via the excited n^4A'', $n > 1$, states—are unimportant relative to mechanism 4. The grounds for this suggestion are dynamic. A trajectory involving the transitions to the energy surfaces of the excited quartet states (those above $1^4A''$) as O^+ approaches N_2 can lead to the evolution of the system to the adiabatic asymptotes of these excited quartet states. For reaction 1 to occur the trajectory would have to pass through a second set of avoided surface intersections in such a fashion as to yield $N(^4S)$, $NO^+(X^1\Sigma^+)$. It is known, on the other hand, that the cross section $\sigma(E_t)$ for the charge exchange reaction

$$O^+(^4S_u) + N_2(X^1\Sigma_g^+) \rightarrow O(^3P) + N_2^+(X^2\Sigma_g^+) \quad (13)$$
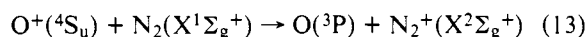
rises rapidly to a constant value for E_t above the thermodynamic threshold and that $\sigma(E_t)$ for reaction 13 is comparable to that for reaction 1 above $E_t \simeq 5$ eV.[38,40] From Figures 5 and 6 it is seen that reaction 13 proceeds by the mechanism reactants $\rightarrow N_2O^+(1^4A'') \rightarrow N_2O^+(2^4A'') \rightarrow$ products. From these results the principal role assigned to the excited quartet states—the production of excited A, BC asymptotic species at the expense of the formation of $N(^4S) + NO^+(^1\Sigma^+)$—is shown to be a very significant role. It is stressed, however, that although a strong negative role vis-a-vis reaction 1 is established for the excited quartet states, present evidence does not suggest that mechanism 5 is insignificant in an absolute sense, but only that it is much less likely than mechanism 4. That the negative role predominates is seen in the rate of decline of the cross section $\sigma(E_t)$ for reaction 1 above its peak as E_t increases. The decline of the experimental cross section is much more rapid than that of a classical trajectory study in which the collisions were constrained to remain electronically adiabatic.[15,16]
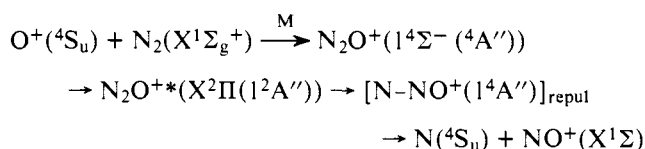
VI. Summary

The mechanisms of the reaction $O^+(^4S_u) + N_2(X^1\Sigma_g^+) \rightarrow N(^4S_u) + NO^+(X^1\Sigma^+) + 1.1$ eV are examined in terms of the electronic states of the triatomic system N_2O^+. Ab initio vertical excitation energies are obtained at both 180 and 130°. A subsequent consideration of the $C_{\infty v}$ and C_s adiabatic correlation of N_2O^+ states to $(N,NO)^+$ and $(N_2,O)^+$ atom–diatom state pairs indicates that adiabatic reaction on the potential energy hypersurface of the $1^4A''$ state is a prominent mechanism.

A survey of the energy surface of the $1^4A''$ state, the only C_s state to which the reactants and products correlate adiabatically, yields a nonlinear saddle-point topology with $(R_{NN}^*, R_{NO}^*, A_{NNO}^*) \simeq (1.28 \pm 0.07$ Å, 1.26 ± 0.07 Å, $120 \pm 5°)$. The position of the saddle point near, or perhaps slightly into, the product side of the reaction coordinate suggests that vibrational excitation of reagent N_2 will be quite effective in promoting adiabatic reaction. The minimum-energy saddle point of the $1^4A''$ surface is situated at 0.1 ± 0.4 eV with respect to the

reagents. Thus, from the ab initio results alone, the $1^4A''$ surface presents either an energy barrier E_b to reaction on the order of 0.1–0.2 eV or no barrier. The adiabatic mechanism is consistent with experimental observation of a two order of magnitude increase in reactivity for reagent excitation *either* translationally beginning at about 0.15 ± 0.05 eV *or* vibrationally excited for $N_2(v)$, $v \geq 2$. The experimental translational threshold is interpreted here to yield a refined barrier value of $E_b = 0.15 \pm 0.1$ eV.

The mechanism for the appreciable, albeit low, reactivity reported experimentally for collision energies below the sharp, strong "threshold" at ~0.15 eV for $N_2(v = 0)$ is different. A calculation of the $(N_2-O)^+$ $1^4\Sigma^-(1^4A'')$ polarization well places its equilibrium geometry at $(R_{NN}^e, R_{NO}^e, A_{NNO}^e) = (1.10 \pm 0.01$ Å, 2.35 ± 0.10 Å, $180°)$ with $D^0(N_2-O^+) = 0.48 \pm 0.1$ eV, $k(N_2-O^+) = 0.33 \pm 0.05$ mdyn/Å, and $\omega(N_2-O^+) = 234 \pm 20$ cm^{-1}. It is shown that the presence of this well enables the interpretation of the low-energy reactivity in terms of the three-step symmetry-allowed but spin-forbidden two-surface mechanism

$$O^+(^4S_u) + N_2(X^1\Sigma_g^+) \xrightarrow{M} N_2O^+(1^4\Sigma^- \, (^4A''))$$

$$\rightarrow N_2O^{+*}(X^2\Pi(1^2A'')) \rightarrow [N\text{-}NO^+(1^4A'')]_{repul}$$

$$\rightarrow N(^4S_u) + NO^+(X^1\Sigma)$$

where it is the *first* step which is rate limiting. For extremely low translational energies (less than about 0.001 eV) the spin-forbidden transition probability at the $(N_2-O)^+$ $1^4A''$–$1^2A''$ intersection is high enough that by-pass of the collisional stabilization step can become important. Other explanations for the prethreshold reactivity cannot as yet be completely ruled out.[9,33] As stated above there may be no barrier in the $1^4A''$ potential energy surface. In this case the low-energy reactivity would result from the lack of a barrier and the "threshold" observed at about 0.1 eV would be due to a dynamic effect. The nature of this effect has been suggested elsewhere.[33] Indeed, both the adiabatic as well as the spin-forbidden mechanism may be operative at low energy.

The mechanism of the state-specific reaction 1 has been of wide interest in recent years because of its key role in ionospheric chemistry. It has become apparent, however, that a complete understanding of the extraordinary mechanistic behavior of reaction 1 will be a significant contribution to the field of gas-phase reaction kinetic theory. Few, if any, atom-diatomic reactions which exhibit a switch from inverse to direct temperature dependence on the one hand and which are governed in large part by a hypersurface favoring noncollinear triatomic conformations in the interaction region on the other hand, are known experimentally. Fewer still are understood theoretically in terms of potential energy surface characteristics. The present report is not final. More ab initio calculations which include polarization functions and wave function correlation are in progress. But also some additional, reliable low-energy scattering and spectroscopic experiments are needed.

References and Notes

(1) (a) Performed in part under the auspices of USERDA under support from the Air Force Office of Scientific Research. This work was begun and largely completed while the author held a National Research Council Postdoctoral Resident Research Associateship supported by the Aerospace Research Laboratories, Air Force Systems Command, 1972–1974. Preliminary reports were presented at the 166th and 170th National Meetings of the American Chemical Society, Chicago, Ill., Aug 1973 and Aug 1975; (b) Address correspondence to Science Applications, Inc., 4124 Linden Avenue, Suite 202, Dayton, Ohio 45432.

(2) See, e.g., A. D. Danilov, "Chemistry of the Ionosphere", Plenum Press, New York, N.Y., 1970, for a discussion; the second most important reaction is $O^+ + O_2 = O_2^+ + O$. Reaction 1 is the principal ionospheric ion–molecule reaction.

(3) C. F. Giese, "Ion-Molecule Reactions in the Gas Phase", *Adv. Chem. Ser.*, **No. 58** (1966).

(4) E. E. Ferguson in "Ion-Molecule Reactions", Vol. 2, J. L. Franklin, Ed., Plenum Press, New York, N.Y., 1972.

(5) E. E. Ferguson in "Interactions between Ions and Molecules", P. Ausloos, Ed., Plenum Press, New York, N.Y., 1975.

(6) A. L. Schemltekopf, F. C. Fehsenfeld, G. I. Gilman, and E. E. Ferguson, *Planet. Space Sci.*, **15**, 401 (1967).

(7) A. L. Schmeltekopf, E. E. Ferguson, and F. C. Fehsenfeld, *J. Chem. Phys.*, **48**, 2966 (1968).

(8) J. C. G. Walker, R. S. Stolarski, and A. F. Nagy, *Ann. Geophys.*, **25**, 831 (1969).

(9) D. K. Bohme, D. B. Dunkin, F. C. Fehsenfeld, and E. E. Ferguson, *J. Chem. Phys.*, **51**, 863 (1969).

(10) A change in mechanism at the minimum in the function $k(T)$ has been suggested by (a) M. McFarland et al., *J. Chem. Phys.*, **59**, 6620 (1973); (b) W. Lindinger, F. C. Fehsenfeld, A. L. Schmeltekopf, and E. E. Ferguson, *J. Geophys. Res.*, **79**, 4753 (1974).

(11) A change in mechanism at the peak of the total cross section function $\sigma(E_t)$ has also been suggested by J. J. Leventhal, *J. Chem. Phys.*, **54**, 5102 (1971).

(12) It has also been suggested that the threshold behavior of the total cross section is due to reaction via excited states above the reagent quartet state by (a) J. J. Kaufman and W. S. Koski, *J. Chem. Phys.*, **50**, 1942 (1969); (b) A. Pipano and J. J. Kaufman, *ibid.*, **56**, 5258 (1972).

(13) See ref 2–5, 6, and 8 for ionospheric temperature data.

(14) R. B. Cohen, *J. Chem. Phys.*, **57**, 676 (1972), finds that for collisions at and above 2.55 eV, vibrational excitation of reagent N_2 has little effect on reactivity, using the total cross section as a reactivity index. Schemltekopf and co-workers, ref 6 and 7, report that vibrational excitation enhances reactivity greatly for $v \geq 2$ for collisions at thermal translational energies, using the rate coefficient as a reactivity index. A quasi-classical trajectory study[15,16] with a surrogate potential surface gives results which agree with the combined results of Cohen and Schmeltekopf et al. in that vibrational excitation is effective only for collisions within 0.75 eV of threshold.

(15) D. G. Hopper, *Bull. Am. Phys. Soc.*, **19**, 261 (1974).

(16) The trajectory studies on surrogate surfaces have been excised from the present report and will be presented in detail as a separate paper. These results have been presented in summary form in ref 15.

(17) R. Johnsen and M. Biondi, *J. Chem. Phys.*, **59**, 3504–3509 (1973).

(18) G. Das and A. C. Wahl, Argonne National Laboratory Report No. ANL 7955, 1972.

(19) D. B. Neumann, H. Basch, R. L. Kornegay, L. C. Snyder, J. W. Moskowitz, C. Hornback, and S. P. Liebmann, POLYATOM (Version 2), Quantum Chemistry Program Exchange, University of Indiana, Program No. 47; see also Program No. 241.

(20) T. H. Dunning, Jr., *J. Chem. Phys.*, **53**, 2823 (1970).

(21) S. Huzinaga, *J. Chem. Phys.*, **42**, 1293 (1965).

(22) The dissociation data collected by F. Gilmore, DNA 1948H, "DNA Reaction Rate Handbook", 2nd ed, 1972, Chapter 10, is perhaps the best available for these diatomics and triatomics.

(23) S. D. Peyerimhoff and R. J. Buenker, *J. Chem. Phys.*, **49**, 2473 (1968).

(24) D. G. Hopper, *Chem. Phys. Lett.*, **31**, 446 (1975).

(25) Several cases are known in which the ab initio SCF total energy is much too high with respect to the SCF total energy of an asymptote. Four examples are given: (a) The SCF energy of H_3 with respect to H + H + H is 0.9 eV higher than the optimized basis/VB-full CI result of −67 ± 1 kcal/mol. See B. Liu, *J. Chem. Phys.*, **58**, 1925 (1973); I. Shavitt et al., *ibid.*, **48**, 2700 (1968); J. M. Walsh and S. A. Matson, *ibid.*, **19**, 526 (1951). (b) The SCF potential barrier for the F + H_2 reaction is 1.4 eV above the experimental activation energy. See C. F. Bender, P. K. Pearson, S. V. O'Neil, and H. F. Schaefer III, *J. Chem. Phys.*, **56**, 4626 (1972). (c) The SCF binding energy for $O_3(^1A_1)$ with respect to $O(^3P) + O_2(X^3\Sigma_g^-)$ is 5.6 (double-ζ basis set) to 4.5 eV (d functions added) too low with respect to the experimental dissociation energy. See P. J. Hay, T. H. Dunning, and W. A. Goddard III, *J. Chem. Phys.*, **62**, 3912 (1975). (d) The SCF energy in the 4s2p basis set for $N_2O(X^1\Sigma^+)$ from ref 26 is within 0.01 eV of the combined energies of its atom + diatomic asymptote $O(^1D) + N_2(X^1\Sigma_g^+)$ from ref 20. The experimental value is 3.8 eV after vibrational correction.

(26) D. G. Hopper in "Potential Energy Surfaces for Air Triatomics", Vol. I, "Literature Review", Vol. II, "Results of SCF and Preliminary OVC Calculations", ARL (AFSC) TR75-0202, June 1975. Available from the National Technical Information Service, Springfield, Va. 22161.

(27) Spectroscopic data has been collected for N_2 by D. C. Jain, *Int. J. Quantum Chem.*, **4**, 579 (1970), and for NO^+ by E. W. Thulstrup and Y. Ohrn, *J. Chem. Phys.*, **57**, 3716 (1972).

(28) J. H. Callomon and F. Creutzberg, *Proc. Int. Conf. Spectrosc., 1st, 1967*, 143–145 (1968); H. M. Rosenstock, *Int. J. Mass Spectrom. Ion Phys.*, **7**, 33 (1971).

(29) G. Herzberg, "Molecular Spectra and Molecular Structure. III. Electronic Spectra and Electronic Structure of Polyatomic Molecules", Van Nostrand-Reinhold, Princeton, N.J., 1966.

(30) L. C. Lorquet and C. Cadet, *Int. J. Mass Spectrom. Ion Phys.*, **7**, 245 (1971).

(31) R. K. Preston and J. C. Tully, *J. Chem. Phys.*, **54**, 4297 (1971).

(32) J. Tully, *J. Chem. Phys.*, **61**, 61 (1974).

(33) L. D. Landau, *Phys. Z. Sowjetunion*, **2**, 46 (1932).

(34) C. Zener, *Proc. R. Soc. London, Ser. A*, **137**, 696 (1932).

(35) E. E. Nikitin in "Chemische Elementarprozesse", H. Hartman, Ed., Springer-Verlag, West Berlin, 1968.

(36) M. Karplus, R. N. Porter, and R. D. Sharma, *J. Chem. Phys.*, **45**, 3871–3873 (1966).

(37) J. T. Muckerman, *J. Chem. Phys.*, **57**, 3388 (1972).

(38) R. F. Stebbings, B. R. Turner, and J. A. Rutherford, *J. Geophys. Res.*, **71**, 771 (1966).

(39) D. K. Bohme, P. P. Ong, J. B. Hasted, and L. R. Megill, *Planet. Space Sci.*, **15**, 1777 (1967).

(40) J. A. Rutherford and D. A. Vroom, *J. Chem. Phys.*, **55**, 5622 (1971).

(41) R. H. Neynaber and G. D. Magnuson, *J. Chem. Phys.*, **58**, 4586 (1973).

(42) G. P. K. Smith and R. J. Cross, Jr., *J. Chem. Phys.*, **60**, 2125 (1974).

(43) (a) Y. Kaneko, N. Kobayashi, and I. Kanomato, *Mass Spectrom.*, **18**, 920 (1970); (b) Y. Kaneko and N. Kobayashi, *J. Phys. Soc. Jpn.*, **36**, 1649 (1974).

(44) T. F. O'Malley, *J. Chem. Phys.*, **52**, 3269 (1970).

(45) J. R. Krenos, R. K. Preston, R. Wolfgang, and J. C. Tully, *J. Chem. Phys.*, **60**, 1634 (1974).

(46) M. L. Vestal and J. H. Futrell, *Proc. 22nd Annu. Conf. Mass Spectrom. Allied Topics*, (1974); private communication, May 1975.

(47) J. Berkowitz and J. H. D. Eland, *J. Chem. Phys.*, **67**, 2740–2752 (1977).

(48) H. S. Johnston, "Gas Phase Reaction Rate Theory", Ronald Press, New York, N.Y., 1966.

(49) R. J. Coleman, J. S. Delderfield, and B. G. Reuben, *Int. J. Mass Spectrom. Ion Phys.*, **2**, 25 (1969).

(50) J. Collin and F. P. Lossing, *J. Chem. Phys.*, **28**, 900 (1958).

(51) A. S. Newton and A. F. Sciamanna, *J. Chem. Phys.*, **44**, 4327–4332 (1966).

(52) V. H. Dibeler, J. A. Walker, and S. K. Liston, *J. Res. Natl. Bur. Stand., Sect. A*, **71**, 371 (1967).

(53) E. E. Ferguson, D. K. Bohme, F. C. Fehsenfeld, and D. B. Dunkin, *J. Chem. Phys.*, **50**, 5039 (1969).

(54) P. G. Orth and R. C. Dunbar, *J. Chem. Phys.*, **66**, 1616 (1977).

Force and Density Study on the Chemical Reaction Process $NH_2 + H \rightarrow NH_3$

H. Nakatsuji,* T. Koga, K. Kondo, and T. Yonezawa

Contribution from the Department of Hydrocarbon Chemistry, Faculty of Engineering, Kyoto University, Kyoto, Japan. Received March 14, 1977

Abstract: Force and density analysis for the radical reaction process $NH_2 + H \rightarrow NH_3$ is given on the basis of the electrostatic force (ESF) theory. We analyze the driving force acting on the approaching H nucleus during the reaction process and investigate the dynamic behavior of the electron cloud from the viewpoint of the electron cloud preceding and incomplete following. The results are: (1) In the initial stage of the reaction, the electron cloud preceding in the atomic region of H, i.e., the inward polarization of the electron cloud, is dominant. The resultant atomic dipole (AD) force gives the predominant contribution to the driving force. However, the stabilization energy due to this AD force is small. (2) In the intermediate stage, the electron cloud preceding occurs as a flow of electron density into the N–H overlap region from the region behind the approaching H nucleus. The electron density thus accumulated in the N–H region gives a large attractive exchange (EC) force. This EC(H–N) force is the dominant driving force of the reaction and gives a predominant contribution to the stabilization energy (heat of reaction) of the system. (3) In the last stage, the repulsive extended gross charge (EGC) force between the undershielded nuclei increases rapidly and terminates the reaction. (4) The addition of the polarization function on the H atom is important to improve the Hellmann–Feynman (H–F) force acting on the H nucleus in the initial and intermediate stages.

Introduction

During the last decade, several force and density studies on the chemical reaction processes have appeared[1,2] on the basis of the electrostatic Hellmann–Feynman (H–F) theorem,[3]

$$\mathbf{F}_A = Z_A \left[\int (\mathbf{r}_{A1}/r_{A1}^3)\rho(\mathbf{r}_1)\, d\mathbf{r}_1 - \sum_{B(\neq A)} Z_B \mathbf{R}_{AB}/R_{AB}^3 \right]$$

(1)

which permits us a simple interpretation of the force through semiclassical electrostatics. Bader and Chandra[4] studied the reaction process $H + H \rightarrow H_2$, analyzing in detail the H–F force and the behaviors of the electron density along the process. They also examined the repulsive He_2 system and compared it with the H_2 system. Chandra and Sunder[5] reported a similar analysis for the formation of the Li_2 molecule and discussed the roles of the core and valence electron densities for the force acting on the nucleus. Nakatsuji, Kuwata, and Yoshida[7] studied the dimerization reaction of two methyl radicals on the basis of the elerostatic force (ESF) theory.[6-9] They have shown that the geometrical change of the reactant,

which is induced by the interaction, would be very important for the occurrence of this reaction. Fukui, Kato, and Fujimoto[10] have studied the reaction coordinate for the substitution reaction $CH_4 + T \rightarrow CH_3T + H$, and analyzed the H–F force in terms of the conventional perturbation theoretic approach to chemical reactions.[11] Curtiss, Kern, and Matcha[12] have calculated the electron density maps for several diatomic alkali halides and analyzed them in relation to the binding and antibinding diagram due to Berlin.[13] Chandra and Sebastian[14a] have recently reported a force analysis for the reaction $He^+ + He^+ \rightarrow He_2^{2+}$, which showed a similar behavior to the previous H_2 system.[4] They have also studied the reactions $He + H^+/He^+ + H \rightarrow HeH^+$.[14b]

Alternatively, we have developed the electrostatic force (ESF) theory for a molecule and interacting molecules and applied it to molecular structures, chemical reactions, and long-range forces.[6-9] In the ESF theory, we have partitioned the H–F force into three pictorial components: atomic dipole (AD) force, exchange (EC) force, and extended gross charge (EGC) force. This partitioning is convenient since they are closely related with the chemical intuitions such as lone pair, bond, and gross charge, respectively. Bader and Jones[15] gave